Pergamon

PII: S0301-9322(96)00046-8

Int. J. Multiphase Flow Vol. 22, No. 6, pp. 1167–1185, 1996

0301-9322/96 $15.00 + 0.00

DETERMINATION OF THE INTERFACE CURVATURE IN STRATIFIED TWO-PHASE SYSTEMS BY ENERGY CONSIDERATIONS

N. BRAUNER, J. ROVINSKY and D. MOALEM MARON

Department of Fluid Mechanics & Heat Transfer, School of Engineering, Tel-Aviv University, Tel-Aviv, 69978, Israel

(Received 17 September 1995; in revised form 18 June 1996)

Abstract—A configuration of a plane interface between two stratified layers is appropriate for two-phase systems which are dominated by gravity, as is the case for large scale air–water systems under earth gravitation. However, for a general two-fluid system, the basic *in situ* configuration is stratified layers with a curved interface. The prescription of the characteristic interface curvature is required in order to initiate the solution of the flow problem and the associated transport phenomena.

Energy considerations are employed to predict the interface configuration. The effect of the fluid physical properties, *in situ* hold up, tube dimension, wall adhesion and gravitation on the characteristic interface curvature are explored. The prediction of interface curvature provides the closure relation required for a complete solution of stratified flows with curved interfaces for a variety of two-fluid systems.

Key Words: stratified flow, interface, curvature, wettability, contact angle

1. INTRODUCTION

The prescription of the free interface configuration in gas–liquid and liquid–liquid systems is of importance in a variety of equipment and processes. For instance, in stagnant two-fluid systems (storage vessels) the interface curvature determines both, the contact area between the phases and wettability distribution of phases with the solid wall. These significantly affect the effective transport phenomena involved.

Of particular importance is the interface curvature in two-phase flow systems. In stratified flow pattern, particularly when the viscosity ratio is high, the interface curvature and its influence on wetted areas may be of crucial effect on the flow pressure drop; for example, the performance of crude-oil/water transportation lines (Russell & Charles 1959; Charles 1960; Charles & Redberger 1962).

Traditionally, the consideration of interface curvature is related to capillary and small scale systems, where the effect of surface tension becomes comparable with gravity. In large scale systems, however, the natural trend is to neglect surface phenomena. This is justified in high density differential systems, such as gas–liquid systems under earth conditions. In liquid–liquid systems with small density difference or in reduced gravity systems (even with high density difference), surface phenomena may dominate, resulting in a curved interface configuration (Brauner 1990). This curved interface may significantly affect the local and integral two-phase flwo characteristics.

So far, stratified two-phase flows studies have assumed plane interface between the phases, which may be reasonable in gas–liquid (air–water) systems (Gemmell & Epstein 1962; Wallis 1969; Taitel & Dukler 1976; Brauner & Moalem Maron 1989; Hall & Hewitt 1993). Previous studies, focusing on liquid–liquid two-phase systems, point out the need to account for phases wettability properties and of the interface curvature in solving for the two-phase pressure-drop, insitu holdup and the stability of the free interface (Russell *et al.* 1959; Bentwich 1964, 1976; Yu & Sparrow 1969; Hasson *et al.* 1970; Brauner & Moalem Maron 1992(a), 1992(b); Barajas & Panton 1993).

In a recent work by the authors (Brauner *et al.* 1996), the two-phase flow characteristics in stratified two-phase systems have been solved for plane and curved interfaces with the interface curvature as a prescribed parameter.

It is the objective of the present study to provide a predictive tool for determining the characteristic interface curvature in two phase systems. The prescription of the interface configuration is a basic input which is needed to further the modeling of two-phase flow problems in a variety of two-fluid systems.

2. DESCRIPTION OF PHYSICAL SYSTEM AND COORDINATES

Consider a horizontal cylindrical conduit occupied with two immiscible fluids in a stable stratification as shown in figure 1. The free interface may approach a plane or lunar configuration depending on the physical properties of the fluids, solid–fluid wettability, the geometrical dimensions and the fluids holdup. The interface may be of convex or concave shape, thus, bipolar coordinate systems are utilized for the circular geometry under consideration. In figure 1, ϕ represents the view angle of the interface from an arbitrary point M in the flow field, represented by radius vectors r_1, r_2 (ϕ is counted in the same direction in both phases, from r_1 to r_2). The pipe perimeter and the interface between the fluids are isolines of coordinate ϕ, so that the upper section of the tube wall, which bounds the lighter phase, is represented by ϕ_0, while the bottom of the tube, which bounds the denser phase, is represented by $\phi = \phi_0 + \pi$. The interface considered to be of cylindrical shape, is defined by $\phi = \phi^*$; it is convex for $\phi^* < \pi$ and concave for $\phi^* > \pi$. In particular, $\phi^* = \pi$ corresponds to the case of plane interface with $h/R = 1 - \cos \phi_0$. The prescription of the ϕ^* is required for solving the hydrodynamic problem (Brauner *et al.* 1996).

In general, when surface effects are significant, the interface configuration tends to attain a convex or concave configuration depending on the relative wettability properties of the two fluids with the wall surface. On the other hand, when gravity is dominant (large density difference), the interface approaches a plane configuration. Global energy considerations are introduced in order to tackle the problem of deriving the interface configuration. For the sake of clarity, energy considerations are demonstrated first in the well-known simple case of free interface formed between two-phases in a vertical tube.

2.1. Energy considerations in vertical tube

Referring to figure 2, the change in the potential energy, surface energy and total energy associated with the rise of a liquid column (from the reference level $H = 0$) are given by:

$$\Delta E_p = \pm(\rho_2 - \rho_1)g\pi R^2 \frac{H^2}{2} \quad [1]$$

$$\Delta E_s = \pm 2\pi RH(\sigma_{2W} - \sigma_{1W}) \quad [2]$$

$$\Delta E = \Delta E_p + \Delta E_s \quad [3]$$

where σ_{1W}, σ_{2W} are the surface tension between the two phases and the solid wall. The upper and lower signs in [1] and [2] relate to $H_m > 0$ and $H_m < 0$, respectively H_m denotes the steady liquid

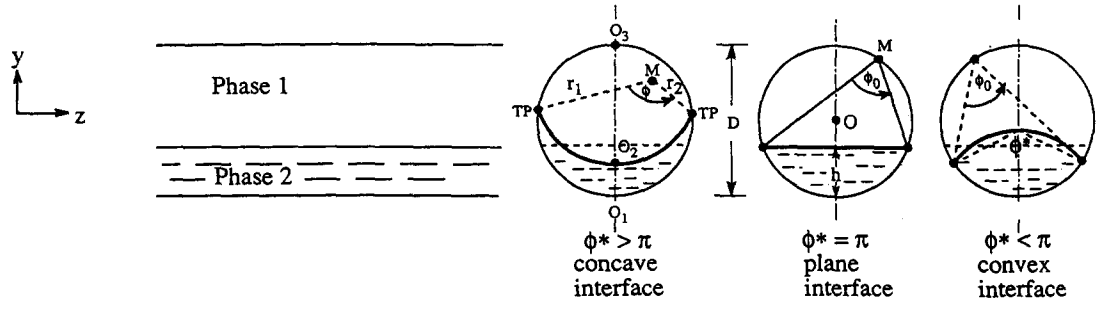

Figure 1. Schematic description of the physical model and coordinate systems.

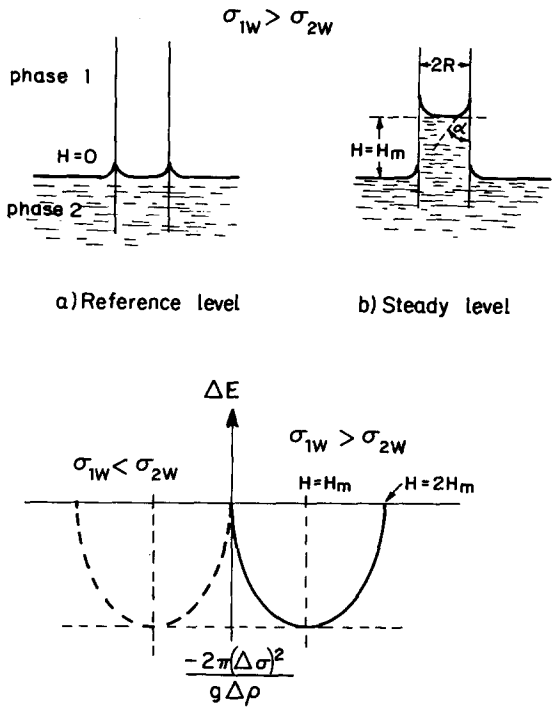

Figure 2. Vertical tube: the steady interface configuration corresponds to a minimum of the total system energy.

level in the tube, see figure 2. Differentiating the total energy change in [3] with respect to the liquid level, H yields that a minimum ΔE is obtained at $H = H_m$

$$H_m = \frac{2(\sigma_{1W} - \sigma_{2W})}{(\rho_2 - \rho_1)gR} = \frac{2\sigma_{12}\cos\alpha}{(\rho_2 - \rho_1)gR} \qquad [4]$$

where σ_{12} is the surface tension between the phases and α is the wettability angle. Note that the Young equation is used in [4] to eliminate $\Delta\sigma_W = \sigma_{1W} - \sigma_{2W}$:

$$\Delta\sigma_W = (\sigma_{1W} - \sigma_{2W}) = \sigma_{12}\cos\alpha. \qquad [5]$$

Thus, for $\Delta\sigma_W > 0$, as the liquid starts climbing from its initial reference state, $(H = 0)$, a reduction in the total system energy takes place for $0 < H < H_m$. This is because the gain in the potential energy, ΔE_p, is smaller than the corresponding loss of surface energy ($\sigma_{1W} > \sigma_{2W}$ as in air/water system, for example).

In the opposite case where $\sigma_{1W} < \sigma_{2W}$ (as may be the case in some oil systems), the increase of the surface energy is initially smaller than the decrease of the potential energy and the minimal of total energy is obtained at $H_m < 0$, corresponding to a physical cases where the liquid drains in the capillary tube below the external reservoir level.

Note that the liquid expression obtained for the steady level of the liquid column via minimal energy consideration given in [4] is identical to that obtained by simple force balance, whereby:

$$\Delta P = (\rho_2 - \rho_1)gH_m = 2\frac{\sigma_{12}}{R}\cos\alpha. \qquad [6]$$

2.2. Energy considerations in a horizontal conduit

The priniciple of predicting the interface location and shape via minimal energy consideration is now applied to the more complicated configuration of a two-phase system in a horizontal cylindrical conduit.

The general relationship for the total energy variation for a unit length of a horizontal tube is given by:

$$\frac{\Delta E}{L} = \frac{1}{L}\Delta(E_p + E_s). \tag{7}$$

The variations of the potential and surface energy terms are calculated with respect to a plane interface (taken as a configuration of reference).

The total change in the potential energy term for the two phases is:

$$\frac{1}{L}\Delta E_p = \frac{1}{L} g(A_1\rho_1 + A_2\rho_2)(YG_{12}^* - YG_{12}^p) \tag{8}$$

where the center of gravity of the two phases with plane interface, YG_{12}^p, and with curved interface, YG_{12}^*, are derived in appendix A in terms of ϕ_0, ϕ^* and insitu holdup ratio, $a = A_1/A_2$.

The total change of the surface energy terms for the two phases is given by:

$$\Delta E_s = (\Delta E_s)_{1w} + (\Delta E_s)_{2w} + (\Delta E_s)_{12} = \sigma_{1w}\Delta S_{1w} + \sigma_{2w}\Delta S_{2w} + \sigma_{12}\Delta S_{12}. \tag{9}$$

Equation [9] represents the change in surface energies involved due to variation of the contact areas of each phase with the solid wall, ΔS_{1w}, ΔS_{2w} and between themselves, ΔS_{12} as the interface switches to its natural curved configuration (from the reference plane configuration). In view of figure A1 (appendix A), the changes in the various contact areas (per unit tube length) are:

$$\frac{\Delta S_{2w}}{L} = 2R(\phi_0 - \phi_0^p) \tag{10.1}$$

$$\Delta S_{1w} = -\Delta S_{2w} \tag{10.2}$$

$$\frac{\Delta S_{12}}{L} = 2R\left[\sin\phi_0 \frac{(\pi - \phi^*)}{\sin\phi^*} - \sin\phi_0^p\right] \tag{10.3}$$

where ϕ_0^p denotes the corresponding ϕ_0 for plane interface.

The surface tension coefficients of the two phases with the solid wall, σ_{1w}, σ_{2w}, are eliminated employing Young formula [5]. Substituting [5] and [10] into [9] yields:

$$\frac{\Delta E_s}{L} = 2R\sigma_{12}\left[\sin\phi_0 \frac{(\pi - \phi^*)}{\sin\phi^*} - \sin\phi_0^p + \cos\alpha(\phi_0^p - \phi_0)\right]. \tag{11}$$

Utilizing [8], [11] for the changes in the potential and surface energies, the total change in the system energy [6] reads:

$$\frac{\Delta E}{L} = \frac{1}{L}(\Delta E_p + \Delta E_s) = R^3\rho_2 g(1 - \tilde{\rho})\left\{\left[\frac{\sin^3\phi_0}{\sin^2\phi^*}(\operatorname{ctg}\phi^* - \operatorname{ctg}\phi_0)(\pi - \phi^* + \sin(2\phi^*)/2) + \tfrac{2}{3}\sin^3\phi_0^p\right] + \epsilon_v\left[\sin\phi_0 \frac{\pi - \phi^*}{\sin\phi^*} - \sin\phi_0^p + \cos\alpha(\phi_0^p - \phi_0)\right]\right\} \tag{12}$$

where, $\tilde{\rho} = \rho_1/\rho_2$ and ϵ_v is the Eotvös number defined by;

$$\epsilon_v = \frac{2\sigma_{12}}{(\rho_2 - \rho_1)gR^2}. \tag{13}$$

The steady interface configuration corresponds to the minimum of the total system energy, $\Delta E/L$. The search for the minimal point of [12] as function of the various physical parameters is discussed in section 3.

3. RESULTS AND DISCUSSION

Before discussing the minimum of [12], it is of interest to analyse separately the variations of the potential and surface energy with the interface curvature. First, the change in the potential energy of the two phases for curved interface, $\phi^* \neq \pi$, with reference to plane interface ($\phi^* = \pi$) is shown in figure 3.

The construction of figure 3 is based on [8] with [A10] for YG_{12}^{P} and [A10]* for YG_{12}^{*} while utilizing the relationship between ϕ_0, ϕ^* and A_1/A_2 as given in [A7] and [A7]*. Note that $\phi^* < \pi$ and $\phi^* > \pi$ represent convex or concave interfaces, respectively. In view of figure 3, any deviation from plane interface results in elevation of the position of the two-phases center of the gravity. Thus, in the absence of surface effects, the minimum of the potential energy also represents a minimum of the total system energy, which is at $\phi^* = \pi$. Hence, in two-phase systems which are absolutely dominated by gravity, a configuration of plane interface is predicted via energy considerations.

The variation of the surface energy with ϕ^*, as given in [11], is demonstrated in figure 4 for the case of $\alpha = \pi/2$, corresponding to identical wettability of the two phases with the solid wall, see [5]. For the case under consideration, the "gain and loss" of the wall energy due to variation of the wall/fluids contact area are equal, and the net change of the total surface energy is merely due to the variation of the interfacial energy between the phases. For the particular case of $A_1/A_2 = 1$, the interfacial area (hence the surface energy as well) is minimal for plane interface, $\phi^* = \pi$. However, for $A_1/A_2 \neq 1$, the interfacial area between the phases increases as the phase of the lower holdup spreads over the wall in a lunar shape, while it decreases when the lower holdup phase shrinks into a convex ("drop") shape. Thus for $A_1/A_2 > 1$, (figure 4(a)), a reduction of the interfacial area takes place as ϕ^* decreases below $\phi^* = \pi$, and the minimal interfacial energy is obtained at $\phi^* < \pi$, corresponding to convex interface. On the other hand, for $A_1/A_2 < 1$ (figure 4(b)), the minimum point is at $\phi^* > \pi$ with concave interface. The value of ϕ^* at the minimum of surface energy varies with the phases holdup ratio, A_1/A_2. In the extreme of $A_1/A_2 \to \infty$, the optimal curvature is $\phi_{op}^* \to 0$ while for $A_1/A_2 \to 0$, $\phi_{op}^* \to 2\pi$.

Figure 5 represents the total surface energy for another particular case of ideal wettability of the lower phase ($\alpha = 0$), for which case [5] becomes $\sigma_{1W} - \sigma_{2W} = \sigma_{12}$. For this case, the reduction of the wall energy, as the lower wetting phase climbs along the wall, is always larger than the

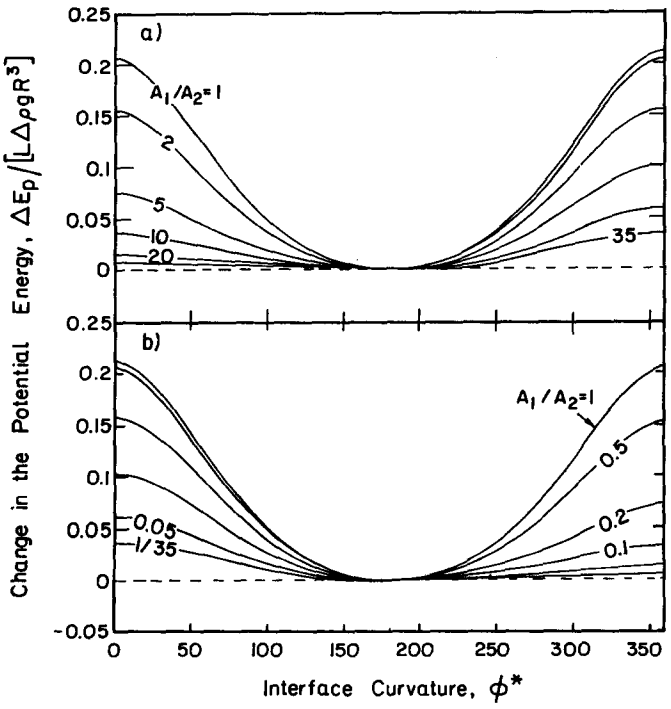

Figure 3. The change in the potential energy associated with variation of the interface curvature.

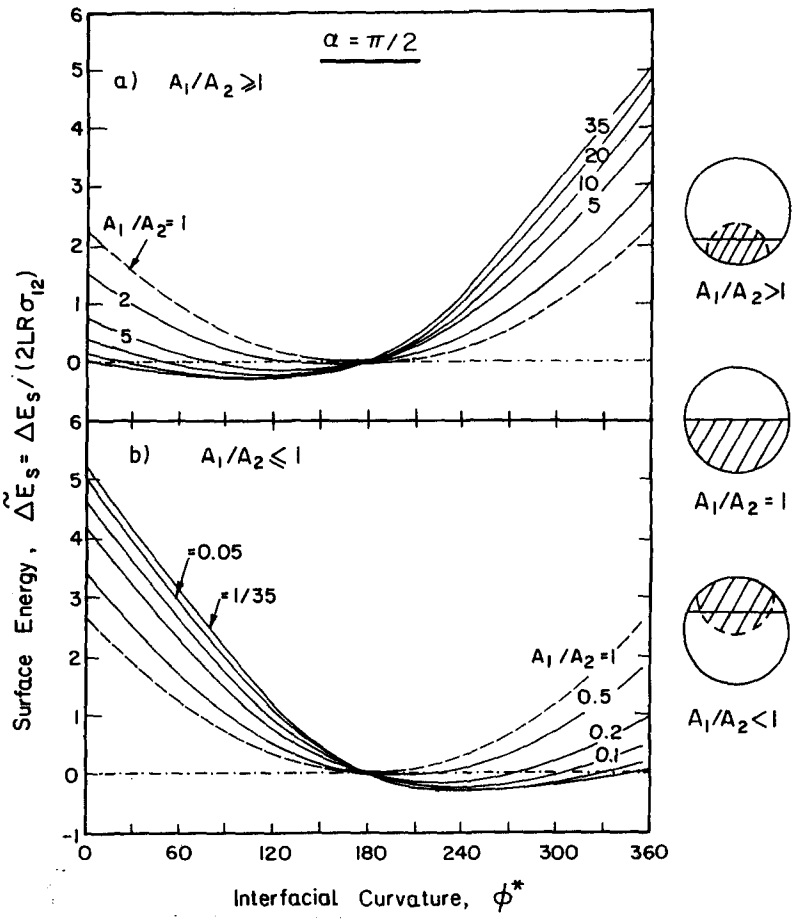

Figure 4. The change in the surface energy associated with variation of the interface curvature, $\alpha = \pi/2$.

associated increase of the interfacial energy. Therefore, the minimal total surface energy is obtained at $\phi^* = 2\pi$. Note that the reduction of the total surface energy with increasing ϕ^* becomes more pronounced as A_1/A_2 decreases. This reflects the fact that for $A_1/A_2 < 1$ and $\alpha = 0$ a concave interface is associated with reduction of both the wall and the interfacial energies (see figure 4).

Complimentary description of the effects of the wettability angle α is shown in figure 6, for $A_1/A_2 = 1$. Again, for $\alpha = \pi/2$ and equal phases insitu holdup, the minimal surface energy is at $\phi^* = \pi$ (plane interface), while for ideal wettability of one of the phases, the minimal surface energy is at either $\phi^* = 2\pi$ for $\alpha = 0$, or $\phi^* = 0$ for $\alpha = \pi$. In general, when the wettability of the wall is more preferable by the lower phase, $0 < \alpha < \pi/2$, the minimum of the total surface energy is obtained at $\pi < \phi^*_{op} < 2\pi$ (concave interface), while for $\pi/2 < \alpha < \pi$, $0 < \phi^*_{op} < \pi$ (convex interface). Obviously, the symmetry in figure 5 is typical of $A_1/A_2 = 1$ only.

Figure 7 represents typical plots of the total energy (potential and surface energies) as a function of the surface curvature, ϕ^*, for a given set of the problem parameters, namely: the wettability angle α, Eotvös number ϵ_v and the phases holdup ratio, A_1/A_2. Note that, given a value of A_1/A_2, ϕ_0^p in [12] is determined by [A7] while the value of ϕ_0 is obtained from [A7]* for each specified value of ϕ^*. With reference to figure 3 (which represents the changes of the system potential energy), the inclusion of the surface energy results in a shift of the location ϕ^*_{op} to ϕ^*_m for which the system total energy is at its minimum. This value of ϕ^*_m represents the ultimate interface curvature at which the phases will stabilize. Thus, ϕ^*_m stands for the predicted steady state interface curvature.

For the particular case of $\alpha = 0$ (ideal wettability of the lower phase), ϕ^*_m is shifted towards values higher than $\phi^* = 180°$, corresponding to a concave interface configuration. This shift increases as the holdup ratio, A_1/A_2, decreases or the Eotvös number increases (see also figure 8). For relatively

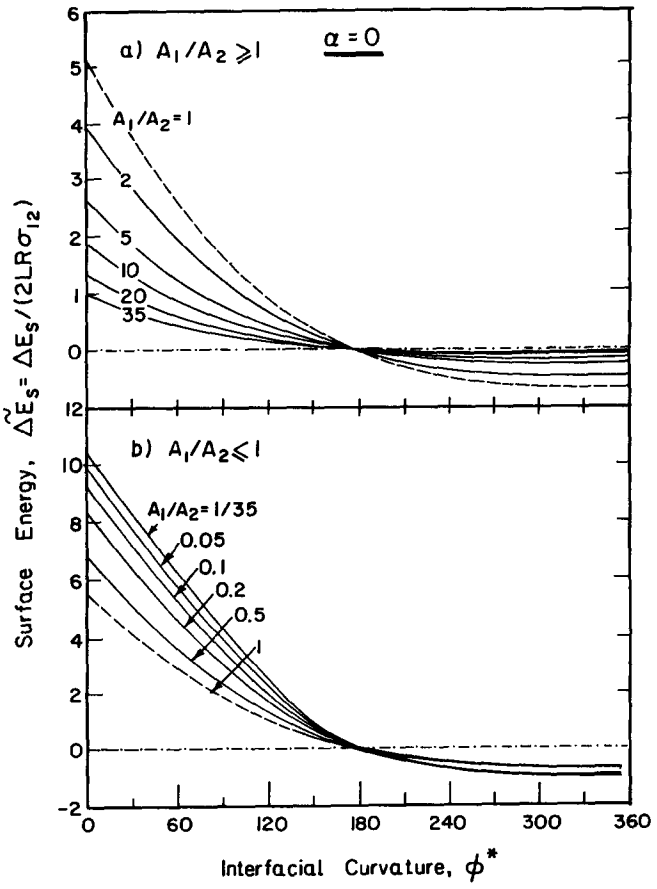

Figure 5. The change in the surface energy associated with variation of the interface curvature for ideal wettability of the lower phase, $\alpha = 0$.

low Eotvös numbers ($\epsilon_v = 10^{-3}$), the curves obained for the total energy are almost identical to those obtained for the potential energy, and the location of ϕ_m^* is close to $\phi^* = \pi$ (plane interface). Obviously for large Eotvös numbers, the total energy curve approaches that of the surface energy.

Figures 8–10 represent a complimentary parametric study on the (optimal) steady interface curvature. In general, for low Eotvös numbers (weak surface energies), the effects of the wettability angle and holdup ratio are moderate. Obviously, for $\epsilon_v \equiv 0$ (the total system energy is identical

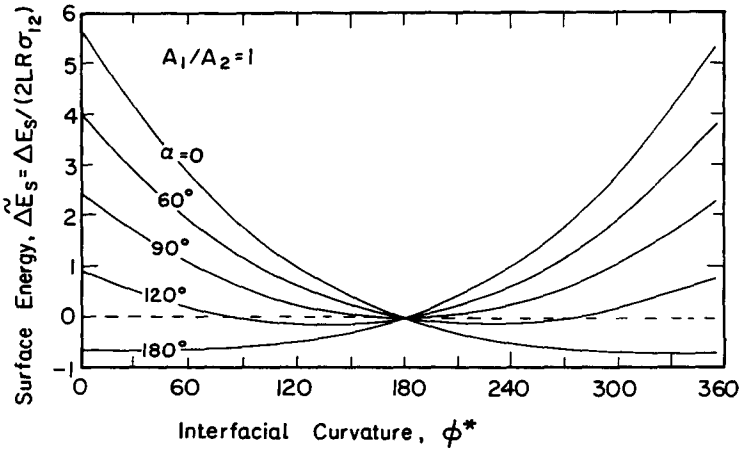

Figure 6. The effect of the phases wettability on the changes of the surface energy associated with variation of the interface curvature.

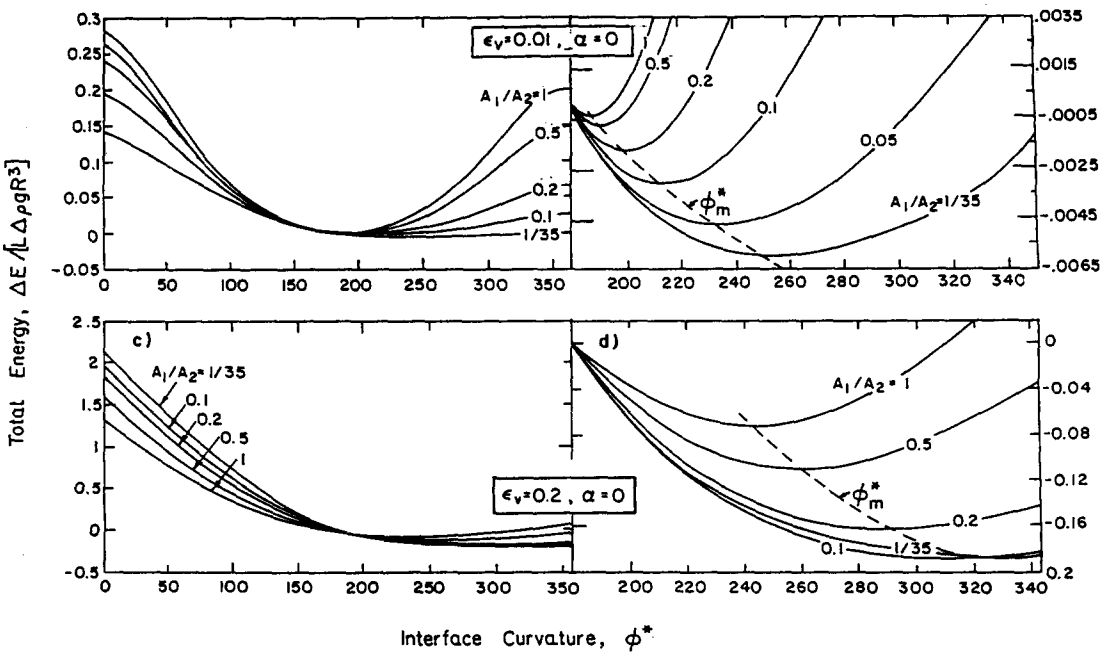

Figure 7. The change in the system total energy associated with variation of the interface curvature.

to the system potential energy) the interface is plane ($\phi^* = \pi$) independent of the phases holdup and wettability angle. However for a finite low Eotvös number and a low holdup ratio (large amounts of lower wetting phase), the steady interface curvature still deviates from plane configuration ($\phi_m^* \neq \pi$) and tends to stabilize in a concave configuration. For instance, air–water systems (which are dominated by gravity) indeed demonstrate a curved liquid interface at sufficiently low gas holdup (gas bubble floating at the upper portion of the pipe). As the Eotvös number increases, dramatic effects of both α and the phases holdup on the interface curvature are expected in view of figures 8(c), (d), 9 and 10.

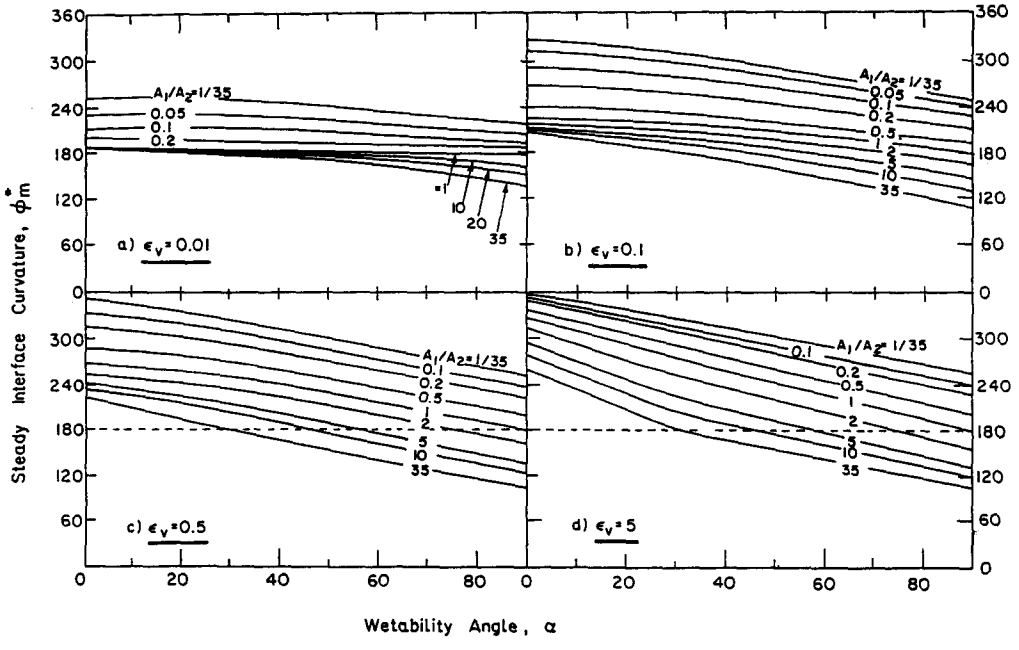

Figure 8. The effect of the phases wettability on the steady interface configuration.

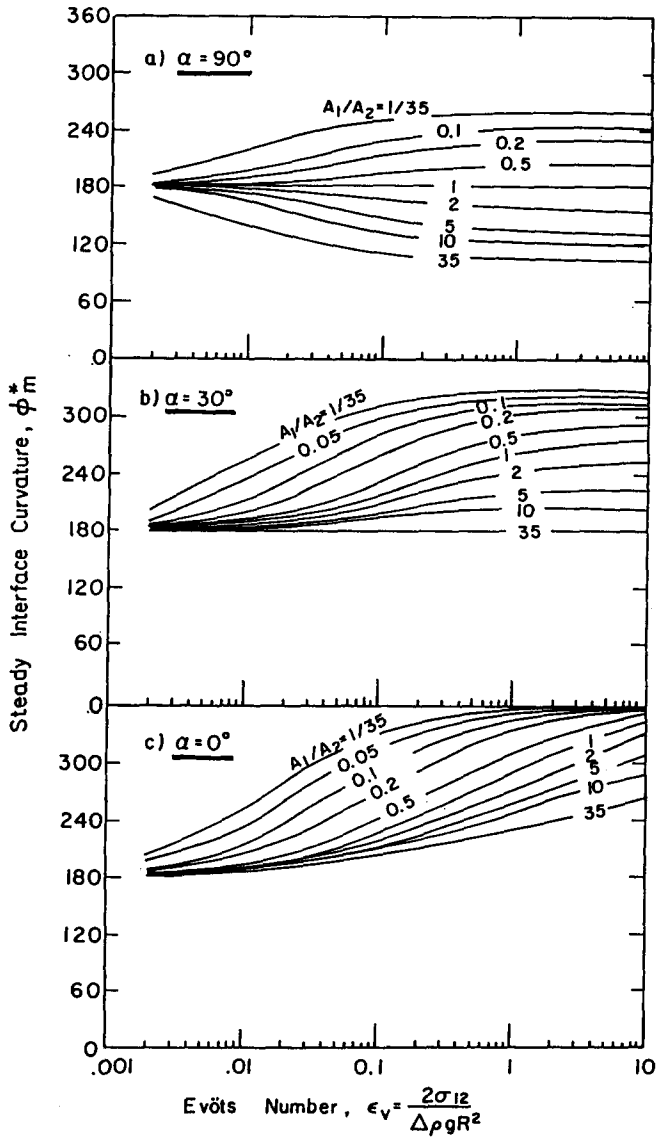

Figure 9. The effect of the system Eotvös number on the steady interface configuration.

It is of interest to note that by varying the wettability, the interface configuration may switch from a concave to a convex configuration. This is well demonstrated at relatively high Eotvös numbers as in figure 8(c), (d). For ideal wettability of the lower phase ($\alpha = 0$), $\phi_m^* \geqslant 180°$ always, thus concave interface is obtained irrespective of the lower phase holdup. In the other particular case of equal wettability, $\alpha = \pi/2$, the interface attains in general a convex configuration for high holdup of the upper phase, and concave configuration for the low holdup range. Hence, at a certain holdup or certain angle of wettability, the interface may demonstrate *convex* configuration although the lower phase is of the higher wettability ($\alpha < \pi/2$).

For sufficiently high Eotvös numbers, $\epsilon_v \gg 1$, the variation of interface configuration with the insitu holdup approaches a uniform curve (independent of the Eotvös value, figure 10). At this range of high Eotvös numbers, the wettability determines the location of the uniform curve of ϕ_m^* as a function of A_1/A_2.

In systems which are dominated by surface effects, $\epsilon_v \to \infty$, the steady interface curvature is determined by the wettability angle and ϕ_0, following simple linear relationship:

$$\phi_m^* = (180 - \alpha) + \phi_0. \qquad [14]$$

The approach of ϕ_m^* towards this limit for $\epsilon_v \gg 1$ is demonstrated in figure 11, obtained for $\epsilon_v = 5$. Thus, in surface tension dominated systems, given the phases wettability angle, the interface configuration (ϕ_0 and ϕ^*) for a certain phases holdup can be easily obained by the intersection point of the straight line [14] with the corresponding holdup curve in figure A2. It is worth noting that for $\epsilon_v \to \infty$, and $\alpha = 0$ (ideal wettability of the lower phase), ϕ_m by [14] coincides with the geometrical upper bound of the solution domain, ($\phi^* = \phi_0 + \pi$, dashed line in figure A2). In this case, the solution obtained for the interface configuration is $\phi_0 = 180°$ and $\phi^* = 360°$, irrespective of the system holdup. This solution corresponds to a floating bubble of the upper phase. For the other extreme of $\epsilon_v \to \infty$ and $\alpha = 180°$ (ideal wettability of the lower phase), $\phi_m^* = \phi_0$, and in view of figure A2, the system configuration is that of a fully eccentric bubble of the lower phase touching the tube bottom. This solution is again independent of the phases holdup. However, for $0 < \alpha < 180°$, when neither of the phases ideally wets the tube wall, the solution for the interface configuration (as obtained from [14] and figure A2) varies with the phases holdup. Thus, even when gravitation is completely absent, partial stratification may take place in the system due to the relative importance of wall energy compared to phases interfacial energy. The interplay between these surface energies in detemining the interface configuration is well understood in view of the discussion that refers to figures 4–6.

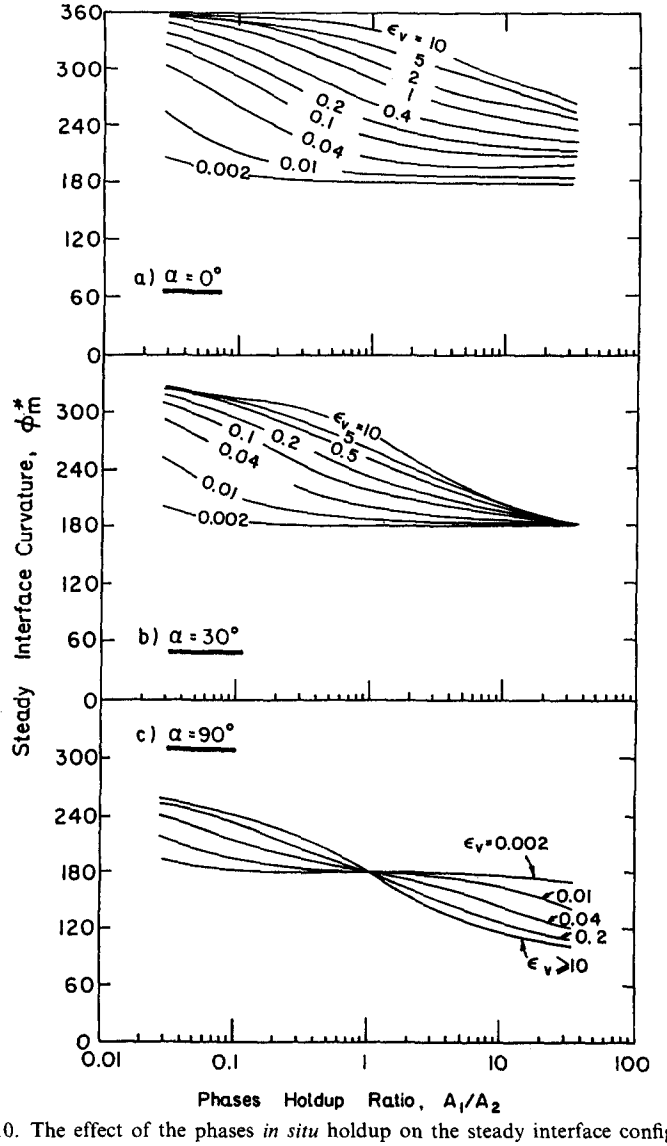

Figure 10. The effect of the phases *in situ* holdup on the steady interface configuration.

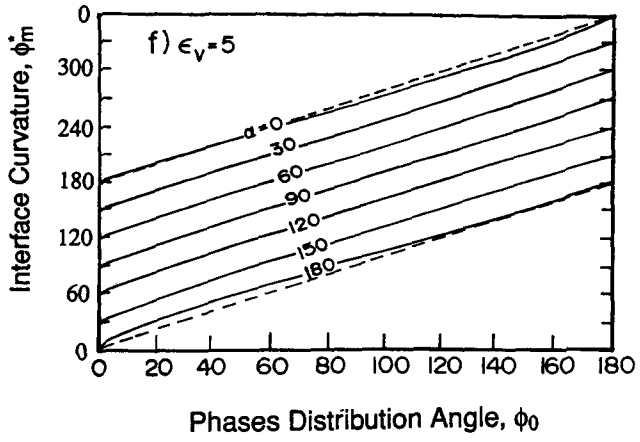

Figure 11. Interface monogram: effect of wall/phases wettability, $\epsilon_v > 1$.

It is to be noted that figures 8–10 summarize the results obtained for the interface configuration as a function of the Eotvös number, ϵ_v, and the phases holdup ratio for the cases where the lower phase is the one of preferable wettability, $0 \leqslant \alpha \leqslant \pi/2$. The steady interface configuration for the cases where the upper phase is the wetting one, $\pi/2 \leqslant \alpha \leqslant \pi$, can be easily obtained from these figures in view of the symmetrical properties of the solutions for ϕ^*_m in the corresponding systems, shown schematically in figure 12.

Given two systems, A and B with the identical ϵ_v number, the interface curvature for system B with $\alpha > 90°$ can be predicted from information obtained for system A with $0 \leqslant \alpha \leqslant 90$, following the rule:

$$\text{When} \quad (\epsilon_v)_B = (\epsilon_v)_A$$

$$\text{and} \quad (\alpha)_B = \pi - (\alpha)_A. \qquad [15.1]$$

Then for $(\phi_0)_B = \pi - (\phi_0)_A$ the interface curvature of system B is given by:

$$(\phi^*_m)_B = 2\pi - (\phi^*_m)_A. \qquad [15.2]$$

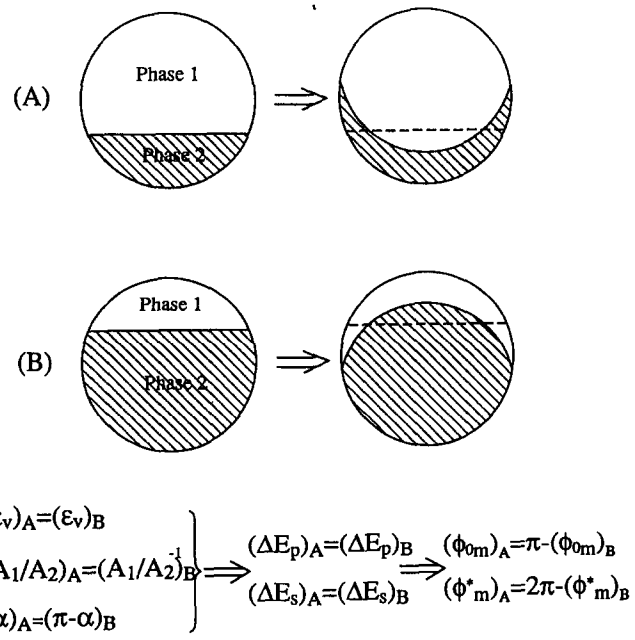

Figure 12. Symmetrical two-phase systems.

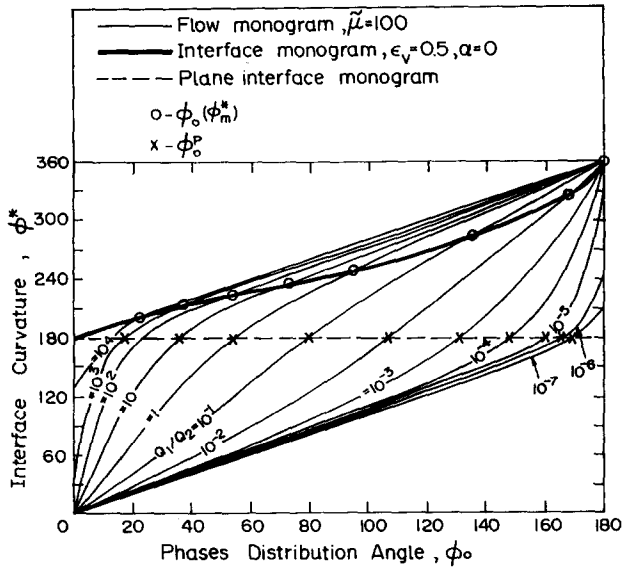

Figure 13. Construction of the system "operational monogram" from the corresponding "interface monogram" and "flow monogram".

The corresponding phases *in situ* holdup in systems A, B are also related whereby $(A_1/A_2)_B = (A_1/A_2)_A^{-1}$.

For comparison, the case of two immisicible fluids contained in a spherical vessel is treated in appendix B. The analytical derivation of corresponding expressions for the changes in the potential energy, surface energy and total energy associated with variations of the interface configuration in spherical geometry are derived and the analogue of [12] is [B9]. The variation of the interface configuration in spherical coordinates follows the same trends as those obtained in cylindrical coordinates when the two geometries are compared at identical phases holdup, Eotvös number and wettability angle.

4. APPLICATION TO THE FLOW PROBLEM

The characteristics of the interface configuration as shown in figures 8–10 are used to construct the so-called *interface monogram*, which is aimed at predicting the steady optimal interface curvature as a function of phases distribution angle ϕ_0 given the phases wettability angle and the system Eotvös number. An example of such an *interface monogram*, is demonstrated in figure 11 and by the bold line in figure 13. The interface monogram presented in the form of ϕ^* as a function of ϕ_0 can be conveniently combined with the hydrodynamic problem, where the *in situ* holdup is determined by the solution of the flow field.

The problem of stratified laminer flow of two phases with a plane or a curved interface has recently been solved by the authors (Brauner *et al.* 1996). The solution for the velocity field of the two-phases V_1, V_2 is obtained in bipolar coordinate system $((\phi, \xi), \xi = \ln(r_1/r_2)$, see figure 1), in terms of Fourier integrals:

$$\frac{V_1}{V_R} = \tilde{V}_1 = 2 \sin\phi_0 \left\{ \frac{\sin(\phi - \phi_0)}{\cosh\xi - \cos\phi} + 2(1-\tilde{\mu}) \frac{\sin(\phi^* - \phi_0)}{\sin(\phi^*)} \int_0^\infty H_{1v}(\omega)\cos(\omega\xi)\, d\omega \right\} \quad [16.1]$$

$$\frac{V_2}{V_R} = \tilde{V}_2 = 2 \sin\tilde{\mu}\phi_0 \left\{ \frac{\sin(\phi - \phi_0)}{\cosh\xi - \cos\phi} + 2(1-\tilde{\mu}) \frac{\sin(\phi^* - \phi_0)}{\sin(\phi^*)} \int_0^\infty H_{2v}(\omega)\cos(\omega\xi)\, d\omega \right\} \quad [16.2]$$

$$H_{1v}(\omega) = \frac{\sinh[\omega(\phi^* - \pi)]}{\psi(\omega)\sinh(\pi\omega)} \frac{\sinh[\omega(\phi - \phi_0)]}{\cosh[\omega(\phi^* - \phi_0)]} \quad [17.1]$$

$$H_{2v}(\omega) = \frac{\sinh[\omega(\phi^* - \pi)]}{\psi(\omega)\sinh(\pi\omega)} \frac{\sinh[\omega(\phi - \pi - \phi_0)]}{\cosh[\omega(\phi^* - \pi - \phi_0)]} \quad [17.2]$$

$$\psi(\omega) = \tanh[\omega(\phi^* - \phi_0)] + \tilde{\mu} \tanh[\omega(\pi + \phi_0 - \phi^*)] \quad [17.3]$$

$$\tilde{\mu} = \mu_1/\mu_2 \quad V_R = \frac{R^2}{4\mu_1} \frac{\partial p}{\partial z}. \quad [17.4]$$

The phases flow rates are obtained by integrating the phases velocities obtained from [16] over the corresponding flow areas A_1, A_2. For a given pressure drop and viscosity ratio, this yields $Q_1(\phi^*, \phi_0)$ and $Q_2(\phi^*, \phi_0)$. The ratio of the two fluids flow rates, is independent of the system pressure drop and is a function of ϕ_0, ϕ^* only. Thus,

$$\frac{Q_1}{Q_2} = \tilde{Q}(\phi_0, \phi^*, \tilde{\mu}) \quad [18]$$

and

$$\frac{\frac{\partial p}{\partial z}}{\left(\frac{\partial p}{\partial z}\right)_{1s}} = \frac{\partial \tilde{p}}{\partial z}(\phi_0, \phi^*, \tilde{\mu}); \quad \left(\frac{\partial p_1}{\partial z}\right)_{1s} = \frac{8Q_1\mu_1}{\pi R^4} \quad [19]$$

The solution of equation [18] can be represented by *flow monogram* curves as in figure 13. In view of the "flow monogram" curves in figure 13, knowing the fluids' flow rates ratio and given the interface curvature ϕ^*, the phases distribution angle ϕ_0 can be extracted which together with ϕ^* determined the *in situ* holdup via [A7] or [A7]*. Thus, each point along the Q_1/Q_2 curve represents a possible combination of (ϕ^*, ϕ_0), corresponding to a certain interface curvature and *in situ* holdup combination. The associated pressure drop is obtained by [19].

The "interface monogram" (as evolves from energy considerations), together with the "flow monogram" (as obtained independently from the hydrodynamic model), constitute the system "*operational monogram*" for a particular set of $(\tilde{\mu}, \alpha, \epsilon_v)$ as demonstrated in figure 13. The intersection between the "interface" and "flow" monograms represents all stratified flows solutions with curved interfaces obtained for varying Q_1/Q_2 ratios. Figure 13 indicates that for a given physical system $(\tilde{\mu}, \alpha, \epsilon_v)$ and operational condition Q_1/Q_2, there exists a single solution (ϕ^*, ϕ_0) which determines the resulting flow characteristics (0 points).

Thus, basically, the input for a stratified flow problem includes the tube geometry, gravitation, flow rates and all the physical properties of the two fluids: viscosities, densities, surface tension and the wall phases wettability angle. Note that the case demonstrated in figure 13 corresponds to a typical oil–water system with $\Delta\rho = 0.1$ gr/cm^3; $D = 1''$ and $\sigma = 40$ dyne/cm, for which $\epsilon_v \simeq 0.5$. But systems of lower density differential (higher ϵ_v) are common in liquid-liquid systems or vapor-liquid systems operating near the critical point. In comparison, the corresponding solution obtained for plane interface (π, ϕ_0^p) is included in figure 13 (denoted by $\times$ points). As is shown for $\alpha = 0$, the discrepancy between (ϕ^*, ϕ_0) and (π, ϕ_0^p) is fairly significant for high Q_1/Q_2 ratios and becomes more and more dramatic for lower Q_1/Q_2 ratios. Another noteworthy point demonstrated in figure 13 is that for a given physical system, a wide range of interfacial curvatures may result with varying the phases input flow rates ratio.

The basic output of an "operational monogram" is the interface configuration corresponding to a particular two-phase system and flow rates ratio associated with this monogram. With the extraction of ϕ^* from the operational monogram, all other two-phase flow characteristics are obtained via the hydrodynamic model (Brauner *et al.* 1996). These include the velocity profiles, interfacial and wall shear stresses distribution and pressure drop. Thus, the prediction of the interface curvature, ϕ^*, becomes an integral part of the complete stratified flow solution.

5. CONCLUSION

The prescription of the characteristic interface curvature is required in order to initiate the solution of stratified flow with a curved interface formed between the phases.

Energy considerations are employed in order to predict the interface configuration. The changes in the system potential energy and surface energies associated with the curving process of the interface are explored. The steady interfacial curvature is shown to correspond to the interface configuration for which the total system energy is at its minimum. Based on this principle, the characteristic interface curvature is predicted as a function of the fluids physical properties, *in situ* holdup, wall/phases wettability angle, tube dimensions and gravity conditions. This provides the "interface monogram" for a particular two-phase system.

The "interface monogram" constitute the closure relation required for obtaining a complete solution of the problem of stratified flow with a curved interface. A convenient frame for obtaining the solution is via the construction of the system "operational monogram", which combines the system "interface monogram" with the system "flow monogram". The latter is obtained from the solution of the hydrodynamic equations for an arbitrary interfacial curvature.

Apparently, the solution of laminar–laminar two-phase flow is determined in terms of two parameters: the phase flow rates ratio and the phases viscosity ratio and is independent of the density differential, surface tension effects, tube dimension or gravitation. This is indeed the case when the flow configuration is restricted to a plane interface between the phases. When this constraint is relaxed, the solution of laminar two-phase flows is shown to be dependent on all of these, and is determined by four nondimensional parameters: phases viscosity ratio, flow rates ratio, wall/phases wettability angle and the Eotvös number. The latter represents the ratio between surface tension and gravity forces.

REFERENCES

Barajas, A. M. & Panton, R. L. 1993 The effects of contact angle on two-phase flow in capillary tubes. *Int. J. Multiphase Flow* **19,** 337–746.

Bentwich, M. 1964 Two-phase axial flow in pipe. *Trans. of the ASME* **86,** 669–672.

Brauner, N. 1990 On the relations between two-phase flows under reduced gravity and earth experiments. *Int. Comm. Heat and Mass Transfer* **17,** 271–181.

Brauner, N. & Moalem Maron, D. 1989 Two-phase liquid–liquid stratified flow. *Physicochem. Hydrodynam.* **11,** 487–506.

Brauner, N. & Moalem Maron, D. 1992(a) Stability analysis of stratified liquid–liquid horizontal flow. *Int. J. Multiphase Flow* **18,** 103–121.

Brauner, N. & Moalem Maron, D. 1992(b) Flow pattern transitions in two phase liquid–liquid horizontal tubes. *Int. J. Multiphase Flow* **18,** 123–140.

Brauner, N., Rovinsky, J. & Moalem Maron, D. 1996 Analytical solution for laminar–laminar two-phase flow in circular conduits. *Chem. Engineering Comm.* **141–142,** 103–143.

Charles, M. E. 1960 The reduction of pressure gradients in oil pipelines: experimental results for the stratified flow of heavy crude oil and water. *Can. Inst. Min. Metal Trans.* **63,** 306–310.

Charles, M. E. & Redberger, P. J. 1962 The reduction of pressure gradients in oil pipelines by the addition of water: numerical analysis of stratified flow. *Can. J. Chem. Engng* **40,** 70–75.

Gemmell, A. R. & Epstein, N. 1962 Numerical analysis of stratified laminar flow of two immiscible Newtonian liquids in a circular pipe. *Can. J. Chem. Engng* **40,** 215–224.

Hall, A. R. & Hewitt, G. F. 1993 Application of two-fluid analysis to laminar stratified oil–water flows. *Int. J. Multiphase Flow* **19,** 711–717.

Hasson, D. Mann, U. & Nir, A. 1970 Annular flow of two immiscible liquids: I. Mechanisms. *Can. J. Chem. Engng* **48,** 514–520.

Russell, T. W. F. & Charles, M. E. 1959 The effect of the less viscous liquid in the laminar flow of two immiscible liquids. *Can. J. Chem. Engng* **37,** 18–34.

Russell, T. W. F., Hodgson, G. W. & Govier, G. W. 1959 Horizontal pipeline flow of oil and water. *Can. J. Chem. Engng* **37,** 9–17.

Taitel, Y. & Dukler, A. E. 1976 A model for prediction flow regime transition in horizontal and near horizontal gas–liquid flow. *AIChE J.* **22,** 47–55.

Wallis, G. B. 1969 *One-dimensional Two-phase Flow*. McGraw-Hill, New York.

Yu, H. S. & Sparrow, E. M. 1969 Experiments on two-components stratified flow in a horizontal duct. *J. Heat Transf. Trans., A.S.M.E.* **91,** 51–58.

APPENDIX A

Geometrical Relationships for Cylindrical System

Consider two-fluid interface (P_1DP_2) as in figure A1. The curved interface is defined by $\tilde{r}$ centered at o_1. In terms of the angles ϕ^* and ϕ_0, the phases cross-sectional areas are given by:

$$A_2 = R^2\left\{\left[\phi_0 - \tfrac{1}{2}\sin(2\phi_0)\right] - \frac{\sin^2\phi_0}{\sin^2\phi^*}\left[\phi^* - \pi - \tfrac{1}{2}\sin(2\phi^*)\right]\right\}; \quad \phi^* \neq \pi$$

$$A_2 = R^2[\phi_0 - \tfrac{1}{2}\sin(2\phi_0)]; \quad \phi^* = \pi \qquad [A1]$$

$$A_1 = \pi R^2 - A_2. \qquad [A2]$$

Note that for specified holdup of the two phases, $A_1/A_2 = a$, [A1] and [A2] yield a relation between a, ϕ_0 and ϕ^*. The center of gravity of the lower phase is given by:

$$YG_2 = \frac{1}{A_2}\int_{A_2} Y\,\mathrm{d}A. \qquad [A3]$$

The center of gravity of the two phases is given by:

$$YG_{12} = \frac{\rho_1 A_1 YG_1 + \rho_2 A_2 YG_2}{\rho_1 A_1 + \rho_2 A_2}. \qquad [A4]$$

Utilizing the fact that for equal densities, $\rho_1 = \rho_2$, the center of gravity is at the tube center, $YG_{12} = 0$, [A4] yields:

$$YG_1 = -\frac{1}{a}\,YG_2. \qquad [A5]$$

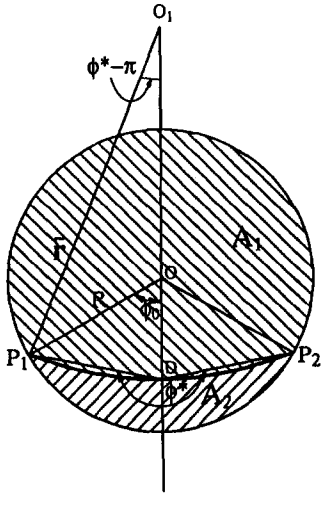

Figure A1. System geometry in polar coordinates.

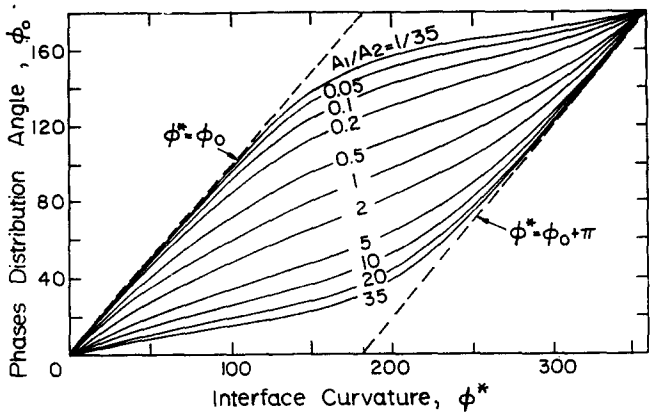

Figure A2. Relation between the interface coordinate, ϕ_0, and its curvature as determined from geometrical considerations.

Clearly, the individual centers of gravity, YG_1 and YG_2 are independent on the phases densities. Therefore, for $\rho_1 \neq \rho_2$, [A5] with [A4] yield:

$$YG_{12} = YG_2 \frac{1-\tilde{\rho}}{a\tilde{\rho}+1}; \quad \tilde{\rho} = \rho_1/\rho_2. \tag{A6}$$

For plane stratified interface, $\phi^* = \pi$

$$\frac{A_1}{A_2} = a = \frac{\pi - \phi_0^P + \frac{1}{2}\sin(2\phi_0^P)}{\phi_0^P - \frac{1}{2}\sin(2\phi_0^P)} \tag{A7}$$

$$YG_2^P = -\tfrac{2}{3}R \frac{\sin^3\phi_0^P}{[\phi_0^P - \frac{1}{2}\sin(2\phi_0^P]} \tag{A8}$$

where ϕ_0^P is the corresponding ϕ_0 for plane interface. In terms of the area ratio (specified holdup) [A8] reads:

$$YG_2^P = -\frac{2R}{3\pi}(a+1)\sin^3\phi_0^P. \tag{A9}$$

Substituting YG_2^P from [A9] into [A6] yields:

$$YG_{12}^P = -\frac{2R}{3\pi}(a+1)\sin^3\phi_0^P \frac{(1-\tilde{\rho})}{(a\tilde{\rho}+1)}. \tag{A10}$$

For curved interface, $\phi^* \neq \pi$

The corresponding expressions are:

$$a = \frac{A_1}{A_2} = \frac{\pi - \phi_0 + \frac{1}{2}\sin(2\phi_0) - \left(\frac{\sin\phi_0}{\sin\phi^*}\right)^2[\pi - \phi^* + \frac{1}{2}\sin(2\phi^*)]}{\phi_0 - \frac{1}{2}\sin(2\phi_0) + \left(\frac{\sin\phi_0}{\sin\phi^*}\right)^2[\pi - \phi^* + \frac{1}{2}\sin(2\phi^*)]} \tag{A7}*$$

$$YG_2^* = \frac{R}{\pi}(a+1)\frac{\sin^3\phi_0}{\sin^2\phi^*}(\operatorname{ctg}\phi^* - \operatorname{ctg}\phi_0)[\pi - \phi^* + \tfrac{1}{2}\sin(2\phi^*)] \tag{A9}*$$

$$YG_{12}^* = \frac{R}{\pi}(a+1)\frac{\sin^3\phi_0}{\sin^2\phi^*}(\operatorname{ctg}\phi^* - \operatorname{ctg}\phi_0)[\pi - \phi^* + \tfrac{1}{2}\sin(2\phi^*)]\frac{1-\tilde{\rho}}{a\tilde{\rho}+1}. \tag{A10}*$$

It can be shown that for $\phi^* \to \pi$, [A7]*, [A9]* and [A10]* converge to [A7], [A9] and [A10].

It is of interest to demonstrate graphically the relationship between the interface curvature, ϕ^*, and the distribution of the two phases contact area with the tube wall (as determined by ϕ_0) for

constant values of insitu holdup ratio, $a = A_1/A_2$. Figure A2 represents the envelope of solutions obtained by [A7] and [A7]* for a wide range of *in situ* holdup ratios. Clearly, given the phases holdup, as ϕ^* increases, the tube surface wetted by the lower phase increases (ϕ_0 increases).

It is worth noting that solutions for $\phi^*(\phi_0)$ are bounded in the range of $\phi_0 \leqslant \phi^* \leqslant \phi_0 + \pi$ (see figure 1). Thus, for $\phi_0 \to 0$, the maximal interface curvature is bounded by π while for $\phi_0 \to \pi$, the minimal curvature is π and its maximal value is 2π. These geometrical bounds are illustrated by the dashed lines in figure A2, which define the envelope for the curves. The dependence of ϕ_0 and ϕ^* (for a given A_1/A_2) is utilized in the calculations of the potential and surface energies variation associated with varying the interface curvature.

APPENDIX B

Spherical Vessel

Two immiscible fluids contained in a spherical vessel are considered (see figure A1). The volumes occupied by the two fluids are given by:

$$V_1 = \frac{\pi R^3}{3}\left[2 + 3\cos\phi_0 - \cos^3\phi_0 + \left(\frac{\sin\phi_0}{\sin\phi^*}\right)^3(2 - 3\cos\phi^* + \cos^3\phi^*)\right]; \quad \phi^* \neq \pi$$

$$V_1 = \frac{\pi R^3}{3}[2 + 3\cos\phi_0 - \cos^3\phi_0]; \quad \phi^* = \pi$$

$$V_2 = \frac{4\pi R^3}{3} - V_1. \qquad \text{[B1]}$$

Hence, for a specified phases holdup ratio, $a = V_1/V_2$, the following relationship for $\phi_0 = \phi_0(a, \phi^*)$ is obtained:

$$2 - 3\cos\phi_0 + \cos^3\phi_0 - \left(\frac{\sin\phi_0}{\sin\phi^*}\right)^3(2 - 3\cos\phi^* + \cos^3\phi^*) = \frac{4}{a+1}; \quad \phi^* \neq \pi$$

$$2 - 3\cos\phi_0^P + \cos^3\phi_0^P = \frac{4}{a+1}; \quad \phi^* = \pi. \qquad \text{[B2]}$$

The center of gravity of the two phases is given by:

(a) For plane interface, $\phi^* = \pi$:

$$YG_{12}^P = \frac{3R\sin^4\phi_0^P}{16}\frac{(a+1)(\tilde{\rho}-1)}{a\tilde{\rho}+1}. \qquad \text{[B3]}$$

(b) For curved interface, $\phi^* \neq \pi$:

$$YG_{12}^* = R\sin\phi_0(\operatorname{ctg}\phi^* - \operatorname{ctg}\phi_0)\frac{(\tilde{\rho}-1)(a+1)}{(a\tilde{\rho}+1)}\left(\tfrac{1}{2} - \tfrac{3}{4}\cos\phi_0 + \tfrac{1}{4}\cos^3\phi_0 - \frac{1}{a+1}\right). \qquad \text{[B4]}$$

The change in the potential energy associated with changing the system configuration—from that of a plane interface to a curved one—is given by:

$$\Delta E_p = \rho_2\frac{4\pi R^4}{3}g(\tilde{\rho}-1)\left\{\sin\phi_0(\operatorname{ctg}\phi^* - \operatorname{ctg}\phi_0)\left[\tfrac{1}{2} - \tfrac{3}{4}\cos\phi_0 + \tfrac{1}{4}\cos^3\phi_0 - \frac{1}{a+1}\right] - \frac{3\sin^4\phi_0^P}{16}\right\}. \qquad \text{[B5]}$$

The associated change in the total surface energies is defined by:

$$\Delta E_s = \sigma_{1W}\Delta S_{1W} + \sigma_{2W}\Delta S_{2W} + \sigma_{12}\Delta S_{12} \qquad \text{[B6]}$$

where:

$$\Delta S_{1W} = 2\pi R^2(\cos\phi_0 - \cos\phi_0^P)$$

$$\Delta S_{12} = \pi R^2\left(\sin^2\phi_0\,\frac{2(\mathrm{ctg}\,\phi^* - \mathrm{ctg}\,\phi_0)}{\sin\phi^*} - \sin^2\phi_0^P\right)$$

$$\Delta S_{2W} = -\Delta S_{1W}. \qquad [B7]$$

Substituting [B7] and Young's equation [5] into [B6] yields:

$$\Delta E_s = 2\pi R^2\sigma_{12}\left[\sin^2\phi_0\,\frac{(\mathrm{ctg}\,\phi^* - \mathrm{ctg}\,\phi_0)}{\sin\phi^*} - \tfrac{1}{2}\sin^2\phi_0^P + \cos\alpha(\cos\phi_0^P - \cos\phi_0)\right]. \qquad [B8]$$

Combining [B5] and [B8] yields the following expression for the total change in the system energy:

$$\Delta\tilde{E} = (\Delta E_p + \Delta E_s)/R^4\rho_2 g(\tilde{\rho} - 1)$$

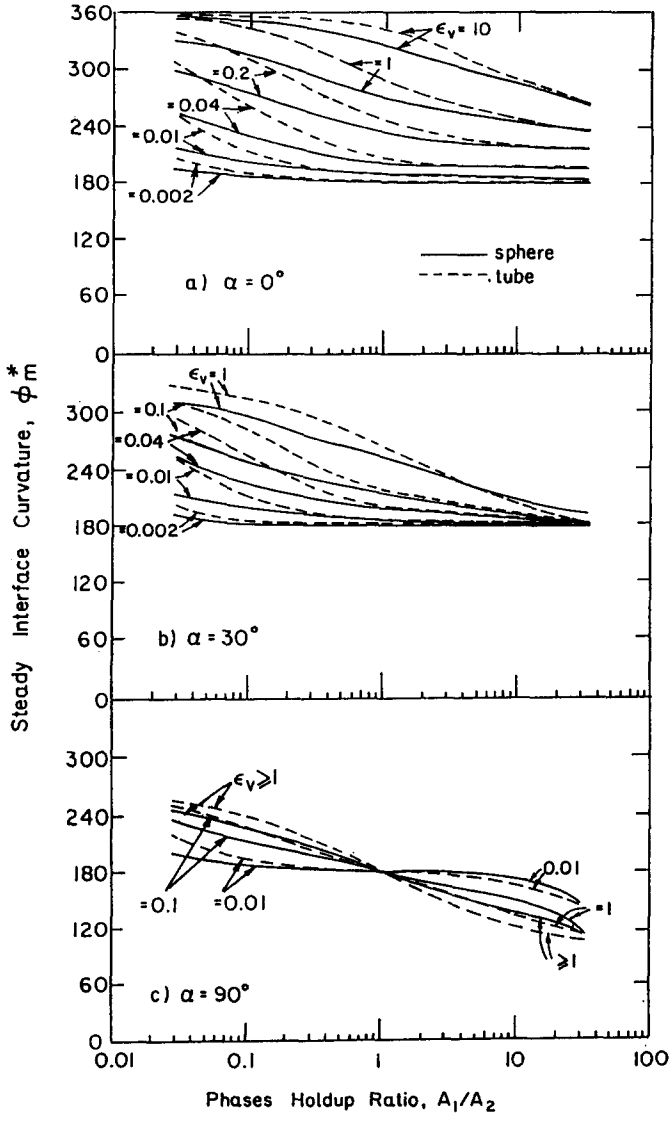

Figure B1. Steady interface configuration: comparison between cylindrical and spherical vessels.

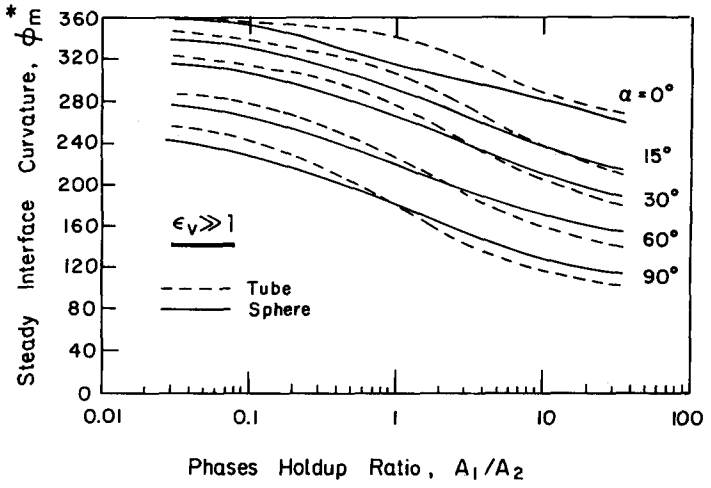

Figure B2. Comparison between the interface curvature in cylindrical and spherical vessels, $\epsilon_v \gg 1$.

$$= \pi\left\{\frac{2}{3}\left[\sin\phi_0(\operatorname{ctg}\phi^* - \operatorname{ctg}\phi_0)\left(\tfrac{1}{2} - \tfrac{3}{4}\cos\phi_0 + \tfrac{1}{4}\cos^3\phi_0 - \frac{1}{a+1}\right) - \frac{3\sin^4\phi_0^P}{16}\right]\right.$$

$$\left. + \epsilon_v\left[\sin^2\phi_0\,\frac{(\operatorname{ctg}\phi^* - \operatorname{ctg}\phi_0)}{\sin\phi^*} - \tfrac{1}{2}\sin^2\phi_0^P + \cos\alpha(\cos\phi_0^P - \cos\phi_0)\right]\right\} \qquad [B9]$$

where ϵ_v is the Eotvös number defined in [13].

Equations [B1]–[B9] can be utilized to produce the analogue curves for all the system variables (ΔE_s, ΔE_p, ΔE) leading to the prediction of the optimal steady interface curvature, ϕ_m^*, in spherical geometry. As the analytical treatment in appendices A and B indicate, the nondimensional parameters representing cylindrical and spherical geometries are identical. These are α, ϵ_v and the *in situ* volume ratio of the phases, V_1/V_2. Note that for the cylindrical case $V_1/V_2 = (A_1L)/(A_2L) \equiv A_1/A_2$.

A summarizing comparison for the optimal steady interface configuration in cylindrical and spherical containers is given in figures B1 and B2. The comparison in figures B1 and B2 is based on identical phases volume ratio in the two geometries. Clearly, for the same two-fluid system, equal Eotvös numbers mean equal containers diameters.

As figures B1 and B2 point out, the general trend of the variation of the interface curvature with the system parameters is similar in both geometries. Moreover, the quantitative gap between the two is reduced as the Eötvos number increases or as the *in situ* volumetric ratio of the less wetting phase increases. For $0 < \alpha \ll 90°$, only at the extreme of low *in situ* ratio, $V_1/V_2 < 0.1$, a cylindrical container demonstrates consistently higher interface curvature.